Published in final edited form as:
Genesis. 2010 December ; 48(12): 693–706. doi:10.1002/dvg.20679.

Widely Expressed *Af17* is likely not required for Embryogenesis, Hematopoiesis, and Animal Survival

Zhijing Zhang[1,4], **Le Huang**[2,4], **Mary Rose Reisenauer**[1], **Hongyu Wu**[1], **Lihe Chen**[1,2], **Yujin Zhang**[3], **Yang Xia**[2,3], and **Wenzheng Zhang**[1,2,5]

[1]Department of Internal Medicine, The University of Texas Health Science Center at Houston, Houston, Texas 77030

[2]Graduate School of Biomedical Sciences, The University of Texas Health Science Center at Houston, Houston, Texas 77030

[3]Department of Biochemistry and Molecular Biology, The University of Texas Health Science Center at Houston, Houston, Texas 77030

Abstract

As a putative transcription factor, Af17 may play a role in multiple signaling pathways. However, the *Af17* expression profile during development and in adult tissues remains largely uncharacterized. The importance of *Af17* function in embryogenesis, hematopoiesis and animal survival has never been addressed before. Here we report the generation of the first *Af17* mutant mouse model, and characterization of the *Af17* temporal and spatial expression profile in various embryonic stages and adult tissues by X-gal staining, in situ hybridization and RT-PCR. *Af17* expression is detected in specific cell populations in all stages and in multiple tissues examined. In situ hybridization yielded a consistent *Af17* expression pattern by X-gal staining. Homozygous mutant mice are viable, fertile, normal in size, and do not display any gross physical, behavioral or hematopoietic abnormalities. Thus, our studies describe the generation of the first *Af17* mutant mouse model, provide the first developmental profile of *Af17* expression, and reveal that *Af17* may be dispensable for normal embryogenesis, hematopoiesis, and animal survival.

Keywords

AF17; MLL6; gene trap; X-gal staining; RT-PCR; leukemia; isthmus; olfactory pit; dorsal root ganglia; central nervous system; brain; kidney; heart; testis; spleen; lung; liver; uterus; eye; bladder; salivary gland; stomach

Introduction

More than 50 genes including *AF9*, *AF10*, and *AF17* have been identified in hematological malignancies as translocation partners of the mixed lineage leukemia gene *MLL* (Bach and Slany, 2009). Such chromosome rearrangements create fusion proteins in which the N-terminal portion of MLL is fused in frame with a part of the fusion partner, destroying the normal histone methyltransferase function of MLL and replacing it with heterologous functions contributed by the fusion partner. The resulting hybrid proteins take control of targets normally controlled by MLL (Slany, 2009).

[5]Address correspondence to: Wenzheng Zhang, Department of Internal Medicine, The University of Texas Medical School at Houston, 6431 Fannin, MSB 1.150, Houston, Texas 77030, Tel: 713-500-6862; Fax: 713-500-6882; wenzheng.zhang@uth.tmc.edu.
[4]These authors contributed equally to this work.

AF17 is one of the earliest identified *MLL* translocation partners (Prasad *et al.*, 1994). Sequence analyses reveal that AF17 belongs to a small family of proteins including human AF10 (Beverloo *et al.*, 1995), BR140 (Thompson *et al.*, 1994) and the Caenorhabditis elegans CEZF protein (Chaplin *et al.*, 1995). These proteins share high homology that is restricted to two regions: the N-terminal plant homeodomain (PHD) finger and the C-terminal leucine zipper. Leucine zippers are often present in many transcription regulators and in some chromatin-associated proteins such as the Moira (Crosby *et al.*, 1999) and histone H3 K79 methyltransferase Dot1 proteins (Okada *et al.*, 2005; Zhang *et al.*, 2004). PHD domains are found in a wide variety of eukaryotic proteins including CBP, MLL, TRX, and Drosophila Polycomb group protein PCL (Lonie *et al.*, 1994; Musselman and Kutateladze, 2009). Thus, AF17 is thought to function as a transcription factor and its PHD domain may be involved in chromatin-mediated gene regulation mechanisms.

Biochemical studies revealed that AF17 is a component of the multisubunit Dot1 complex (Dotcom), which harbors several MLL partners such as ENL, AF9, AF10, and AF17, as well as the known Wnt pathway components TRRAP, Skp1, and β-catenin (Mohan *et al.*). These studies imply that AF17, as a component of the DotCom, plays a role in the Wnt/Wingless signaling pathway. AF17 also seems to be a downstream target of the β-catenin/T-cell factor pathway, and plays a role in G2-M progression (Lin *et al.*, 2001). Our recent investigation indicates that AF17 competes with AF9 to bind with Dot1a in the aldosterone signaling pathway and upregulates transcription of multiple genes, including those encoding the epithelial Na^+ channel (ENaC) subunits α, β, and γ (Reisenauer *et al.*, 2009). Therefore, AF17 is thought to function as an important regulator of ENaC-mediated Na^+ transport and thus blood pressure.

Although *AF17* is involved in multiple signaling pathways, very little is known regarding the *AF17* temporal and spatial expression profile during embryonic development and in adult tissues. Northern blot analysis demonstrated the presence of *Af17* mRNA in brain, heart, kidney, lung, muscle, and stomach, but not in liver, of P17 (17 days postnatal) mice (Kleiter *et al.*, 2002). The role of Af17 in normal hematopoiesis is virtually unknown. Furthermore, to our knowledge, no *Af17* mutant mouse models have been reported. Therefore, we generated the first *Af17* mutant mouse model using a gene trap approach, and characterized *Af17* expression profile in a variety of tissues/organs in several developmental stages varying from E10.5 to adulthood using X-gal staining, in situ hybridization and RT-PCR. Thus, our studies not only provide the first spatiotemporal expression profile of *Af17*, but also describe the generation of the first *Af17* knockout mouse model as a valuable agent to elucidate in detail the in vivo function of *Af17*.

Results

Generation and characterization of *Af17*$^{-/-}$ mice

We created *Af17* mutant mice by using an existing gene trap embryonic stem (ES) cell line derived from strain 129OLA (GenBanK#: CW988924). We chose this clone from 11 available *Af17*-specific candidate ES lines because its insertion site is closest to the 5' end of *Af17* gene, allowing maximal disruption of the *Af17* transcribed region. Alignment of *Af17* cDNA (GenBank# AY050217) and the mouse genomic sequences revealed that the gene trap vector (pGT0lxr) was inserted into intron 7. The insertion disrupts *Af17* mRNA splicing between exon 7 and 8, presumably leading to deletion of Af17 aa 256-1079 and generation of a hybrid protein harboring Af17 aa 1-255 fused in-frame with β-geo reporter (Fig. 1A). Thereby, the fusion protein expression is under control of the endogenous *Af17* promoter, allowing determination of *Af17* expression profile by X-gal staining. Furthermore, the insertion is also expected to remove most, if not all, of the Af17 function. In particular, the

hybrid protein harbors the PHD finger (aa 8-58), but is not anticipated to bind Dot1a because it lacks the Dot1a-interacting domain (aa 635-786) (Reisenauer *et al.*, 2009).

After sequencing a genomic PCR fragment spanning the junction, the exact insertion site was found 257 bp downstream from the start of intron 7 (GenBank # GU271153). The ES clone was used to generate chimera mice. Chimeric animals were crossed with C57BL/6 mice to generate F1 offspring. Mice from inbred F5-F10 generations were generated and used for the current studies.

Genotyping was conducted by PCR of genomic DNA with primers located upstream and downstream of the insertion site within intron 7 as well as the vector sequence upstream of the coding region of the reporter (P2, P3 and P5, Fig. 1B). To determine whether *Af17* mRNA had been inactivated, as well as to confirm that the β-geo reporter was expressed, total brain RNA was isolated and analyzed by RT-PCR with primer pairs specific for WT or mutant *Af17* transcripts. As shown in Fig. 1C, RT-PCR with exon 7-and β-geo-specific primers (P1 and P4) demonstrates that the mutant mRNA is undetectable in WT control, but readily amplified in $Af17^{-/-}$ animals. Reciprocally, RT-PCR reactions with another set of primers (P6 and P7) encoding Af17 aa 883-890 and aa 1041-1049, respectively, generated the expected 498-bp fragment from WT but not mutant mice (Fig. 1C). Similarly, PCR with primers P1 and P4 revealed that the mutant mRNA was also expressed in kidney, testis, eye, bladder, heart, lung, spleen, but not liver of the $Af17^{-/-}$ mice. Parallel PCR with primers P6 and P7 did not yield detectable WT products in these tissues (Fig. S1). X-gal staining of $Af17^{-/-}$ liver (Fig. 6A) and RT-PCR of $Af17^{+/+}$ liver (Fig. 6B) further confirmed little or no Af17 expression in this tissue. To confirm the expression of β-geo at the protein level, Western blot analysis of whole lysate from kidney, brain and heart with an antibody against β-gal was performed. An ~120 kd band was consistently found in these tissues only from mutant mice, but absent in those from all WT mice examined (Fig. 1D). This band is smaller than the predicted size (~170 kd) of the fusion protein, presumably due to post-translational cleavage. In brief, these results together with data presented below demonstrate that WT animals express *Af17* mRNA, and mutant mice harbor the disrupted *Af17* genomic sequence and express the mutant allele at both mRNA and protein levels in their brains and all other tissues examined, with no or little Af17 expression in liver. We aggressively pursued the verification of the absence of WT Af17 proteins in $Af17^{-/-}$ mice. Unfortunately, as we recently reported (Reisenauer *et al.*, 2009), all three commercial antibodies against Af17 failed to specifically detect the endogenous Af17 by immunoblotting, immunohistochemistry, or immunofluorescence analyses. Similarly, our newly developed Af17 antibody also failed in parallel experiments (data not shown). In fact, to our knowledge, detection of the endogenous or overexpressed full-length Af17 proteins by these methods has never been reported in the literature.

$Af17^{-/-}$ animals are viable and have neither significant growth retardation nor leukemia

Af17 is not apparently required for normal embryogenesis and animal survival as evidenced by the existence of homozygous mutant animals. These animals appear to be healthy and fertile. We summarized the number of all live pups resulting from crosses between $Af17^{+/-}$ heterozygotes six weeks after birth based on their genotypes. The ratio among the three genotypes is not significantly biased from the expected 1:2:1 Mendelian ratio (data not shown). A detailed growth curve analysis starting from day 6 to day 34 after birth indicates that the three genotypes share a very similar growth curve, although $Af17^{-/-}$ mice displayed a slight, but not statistically significant growth retardation during day 16 to 28 (Fig. 2A).

Since AF17 is a fusion partner of MLL, we questioned if Af17 is required for normal hematopoiesis and if loss of *Af17* function is leukemogenic. For this purpose, peripheral blood smears of multiple $Af17^{-/-}$ animals were examined. As shown in Fig. 2B, peripheral

blood cells have normal morphology and no leukemic cells were present in the *Af17*$^{-/-}$mice. Complete blood count revealed a normal range of each parameter of red blood cells, white blood cells, and platelets. For example, total hemoglobin and hematocrit were not significantly different from WT in the adult *Af17*$^{-/-}$ mice (Fig. 2C-E). Consistent with these observations, the bone marrow cells of WT adult animals did not show detectable *Af17* mRNA expression by RT-PCR (Fig. 6). Similarly, no X-gal staining was observed in the bone marrow cells of *Af17*$^{-/-}$ mice (data not shown). These results suggest that *Af17* is apparently not required for normal hematopoiesis and loss of *Af17* function does not cause any obvious phenotype associated with leukemia, at least by 6-8 weeks after birth. However, further studies are required to determine if *Af17*$^{-/-}$ mice develop leukemia with age.

Af17 is expressed in the embryonic nervous system

The viability of *Af17*$^{-/-}$ mice provides an excellent opportunity to examine the *Af17* expression during embryonic stages and in adulthood by X-gal staining. Accordingly, we first collected embryos and conducted whole mount X-gal staining at various stages from the three genotypes. The earliest embryonic stage when β-gal activity was examined is E10.5 day. At this stage, *Af17*$^{-/-}$ mice showed X-gal staining in the midbrain-hindbrain junction (isthmus), margin of the olfactory pit, and the rostral end of the forebrain around the dorsal midline. Relatively weak staining could also be seen at the edge of the forelimb bud and the tail bud (Figs. 3A and B). The same pattern of X-gal staining was observed in *Af17*$^{+/-}$animals, but weaker (data not shown). Wild type embryos showed no background staining, indicating the absence of the endogenous β-gal activity at this stage (Fig. 3C). To further identify the *Af17*-expressing tissue types, we made sagittal sections through the neural tube. On the sections, it is clear that the expressing tissue is the neuroepithelium, but not adjacent mesoderm or ectoderm (Fig. 3D).

Whole mount X-gal staining of E12.5 day embryos revealed that the *Af17*-expressing area expanded in the central nervous system (CNS, Fig. 4). From the isthmus, it extended rostrally towards the forebrain along the dorsal midline of the midbrain. Caudally from the isthmus, faint staining was seen along the midline of the neural tube and dorsal root ganglia on both sides of the developing spinal cord (Figs. 4A and B). In the forebrain, expression areas included the median walls of telencephalic vesicles and the nasal epithelium (Figs. 4C). Moreover, this time point was the first time that the developing eye started to express *Af17* (Fig. 4D). Similar to E10.5 day embryos, no background X-gal staining was observed in wild type embryos (Figs. 4E).

We then sectioned those X-gal stained embryos to visualize the internal structures. Since the retinal pigmented epithelium has already developed at this stage and its very dark color obscures X-gal staining, we also made sections of the optic vesicle for better visualization of the eye primordium. In this way, *Af17* expression was confirmed in the median walls of the telencephalic vesicles (Fig. 4F), and in the optic cup with the basal (lens) side of the neural retina being stained to a greater extent (Fig. 4G).

At the developmental stage of E14.5 day, the E12.5 expression pattern was basically maintained. Compared with earlier stages, the expression in the dorsal root ganglia becomes more obvious (Fig. 4I). The specificity of the staining was supported by the fact that WT embryos at this stage remained non-reactive to X-gal staining (Fig. 4J). Transverse sections helped us to confirm these structures as the dorsal root ganglia (Figs. 4K and L).

Af17 is expressed in the embryonic heart and kidney

Af17 is also expressed outside of the nervous system during embryonic development. In E12.5 day whole mount embryos, we observed X-gal stained internal structures. To reveal

the nature of these structures, we made sagittal sections of the embryos and found that *Af17* was highly expressed in the heart and the metanephro. Some staining can be found in the regressing mesonephro, mainly along the mesonephric tubules (Fig. 4H).

Af17 is expressed in multiple organs at late embryonic stages

At a late embryonic stage (E16.5 day), organs were dissected out to facilitate fixation and subsequent X-gal staining. In *Af17*$^{-/-}$ embryos, staining was clearly seen in the brain, kidney, testis, heart, and lung. Weaker staining was detected in the bladder and stomach. The spleen and liver were devoid of *Af17* expression. X-gal staining was also observed in the eye, but well-developed pigmented tissue makes it difficult to visualize the blue staining in this picture (Fig. 5). A similar pattern of X-gal staining was observed in *Af17*$^{+/-}$ embryos. However, like in early stages, the staining was weaker compared to homozygous mutant embryos (Fig. 5). Furthermore, no noticeable background X-gal staining was seen in any of these organs except kidney of the WT control (Fig. 5).

Af17 is expressed in multiple organs in the adult mouse

To study the expression pattern of *Af17* in adult organs/tissues, we performed whole mount organ staining using both WT and *Af17*$^{-/-}$ animals at 6 to 8 weeks of age. The pattern of X-gal staining in *Af17*$^{-/-}$ mice was reminiscent of that seen at E16.5, as evidenced by the continued high level of *Af17* promoter activity in brain, kidney, testis, eye, bladder, and heart, and no detectable staining in liver. Unlike at E16.5, pronounced staining was also found in spleen. Whole mount X-gal staining analyses of additional organs identified salivary gland and uterus as positive and small intestine and penis as negative for *Af17* expression (Fig. 6A). In all cases except brain, heart, liver, and penis, all other organs isolated from WT animals also showed background X-gal staining, most likely due to the presence of endogenous β-gal activity (Fig. 6A).

In addition, the dark colors of some organs disguise the blue color of X-gal staining, which is particularly problematic for whole mount organ staining; for example, spleen and kidney present this difficulty (Fig. 6A). Accordingly, we performed RT-PCR to detect the endogenous *Af17* mRNA expression in these organs collected from wild type animals, with β-actin as positive control and reactions omitting reverse transcriptase as negative control. As shown in Fig. 6B, no PCR products were generated with primers either specific for *Af17* or *β-actin* in the negative control reactions, ruling out the possibility of genomic DNA contamination. In the presence of reverse transcriptase, a primary band with the correct size of the predicted *Af17* fragment was repeatedly amplified in all organs except for small intestine and bone marrow, confirming and extending the X-gal staining results.

Two points should be noted. First, additional fragments of various sizes ranging from 300-1000 bp were simultaneously amplified, possibly due to extensive alternative splicing at the 3' end of *Af17* gene, similar to results we reported for Dot1 (Zhang *et al.*, 2004). Alternatively, these products may have been generated non-specifically due to sub-optimal RT-PCR conditions. However, this is unlikely because they were only observed in a subset of tissues such as kidney, eye, bladder, heart, and lung, and barely detectable in other organs including spleen. Further analyses are required to reveal the identities of these products. Obviously, such alternative splicing events, if they exist, occur in a tissue-specific manner. Secondly, although these multiple unidentified products have prevented us from performing real-time RT-qPCR to determine the relative *Af17* mRNA levels across the tissues, the proportionate band intensity of the primary product largely correlates with the X-gal staining. For example, liver, small intestine, and penis yielded undetectable or very faint signals in both X-gal staining and RT-PCR analyses. However, lung gave inconsistent results. *Af17* expression was apparently high as detected by RT-PCR, but undetectable by X-

gal staining. We do not know the exact reasons for this discrepancy. Because Northern blot analysis also revealed expression of *Af17* mRNA in P17 lung (Kleiter *et al.*, 2002), it can be speculated that the Af17-β-geo fusion was somehow degraded or its β-gal activity inactivated specifically in this adult tissue, and became undetectable by X-gal staining, although it was expressed at mRNA level. Similar inconsistency has been reported for Af9 expression in the Af9lacZ transgenic mice. The adult central nervous system of these animals lacked detectable Af9 mRNA expression, yet showed extensive X-gal staining, possibly due to the stability of the β-gal protein and an accumulation of the protein during development (Vogel and Gruss, 2009). Finally, *Af17*$^{-/-}$ mice apparently do not express detectable WT transcripts as evidenced by a lack of the expected PCR product with primers P6 and P7 in all tissues examined (Fig. S1), indicating that the 3' splicing variants (if any) are most likely disrupted by the insertion of the gene trap vector.

Af17 is expressed in subpopulations of neurons in the adult brain

The Drosophila homolog of AF10/AF17 genes (*Dalf*) is highly expressed in the nervous system (Bahri *et al.*, 2001). Similarly, we found that *Af17* promoter activity is readily detected in the whole mount adult brain. To ensure reliable detection of β-gal activity in deep structures, brains of 6-8 week-old *Af17*$^{-/-}$ mice were dissected out and quickly frozen in liquid nitrogen. Cryosections were made, followed by fixation and X-gal staining performed on the slides. The X-gal staining pattern strongly suggests that *Af17* expression is limited to some specific brain areas. For example, in the forebrain, X-gal staining was detected in the cerebral cortex, hippocampus and some deep nuclei (Figs. 7A, B, and B'). Such specificity is further highlighted by a large contrast in staining intensity in closely related structures; for example, the hippocampal cornis ammonis (CA) areas show strong staining but the hippocampal dental gyrus shows almost complete absence of staining (Figs. 7B and B'). Similarly, in the cerebellum, X-gal staining is prominent in the molecular layer but absent from the granular layer despite the very high cell density present in this layer (Fig. 7C and D).

The nervous system mainly consists of glial cells and neurons. To identify the cell type expressing *Af17* in the adult brain, we performed X-gal staining, followed by immunohistochemical (IHC) labeling using antibodies against glial fibrile acidic protein (GFAP) and NeuN: two well-characterized markers for astrocytes and neurons, respectively (Eng *et al.*, 2000; Mullen *et al.*, 1992). We examined multiple areas including those mentioned above, and consistently found that X-gal positive cells were not co-labeled by anti-GFAP antibody (Figs. 7E and F), indicating that they were not astrocytes. In contrast, the expression patterns of *Af17* and NeuN were largely, but not completely overlapping, as shown in the pyramidal cell layer of hippocampus (Figs. 7G & H) and the cerebral cortex (Figs. 7I & J).

While the majority of *Af17*-expressing cells are NeuN-positive neurons, a small portion of X-gal stained cells were not reactive to the anti-NeuN antibody, implying that *Af17* is also expressed in some non-neuronal, non-astrocytic cells such as oligodendrocytes. However, based on the fact that many types of neurons have been identified as NeuN-negative (Mullen *et al.*, 1992), it is also likely that *Af17* is expressed in neurons but these neurons are NeuN-negative. Furthermore, some NeuN-labeled cells were devoid of X-gal staining, suggesting that *Af17* expression occurs only in a subpopulation of neurons. In brief, we conclude that most, and perhaps all *Af17* expressing cells in the adult brain are neurons.

Hematoxylin & Eosin staining of brain sections did not reveal any noticeable morphological difference between WT and *Af17*$^{-/-}$ animals (Figs 7K to N). In addition, We have not observed any overt behavioral abnormalities in the mutant mice.

In situ hybridization (ISH) for Af17 mRNA and X-gal staining demonstrated similar expression patterns

To test if the X-gal staining in our gene-trap model can faithfully represent the endogenous expression of the *Af17* gene, ISH was performed to confirm the X-gal staining results. ISH was performed with sense and antisense probes specific for Af17 toward WT E17.5 embryos. We first focused on the area around the spinal cord and dorsal root ganglia because these structures are easily recognized and, based on previous X-gal staining, the contrast between expressing tissues and their surrounding tissues is clear.

X-gal staining revealed high β-gal activity in the DRG and, to a lesser degree, in the spinal cord (Figs 8A-C). ISH with an antisense probe encoding Af17 aa 237-387 yielded a similar staining pattern showing signals in the spinal cord and DRG; however, the difference between the DRG and the spinal cord is not obvious (Fig. 8D). The lesser contrast seen may reflect a higher sensitivity of the ISH method than X-gal staining. When the corresponding sense probe was used, only background signal was observed, demonstrating the high specificity of the ISH method (Fig. 8E).

Another organ that we examined by both X-gal staining and ISH is the kidney. At E17.5, β-gal activity is sparsely detected in the cortex and medulla of the $Af17^{+/-}$ mice (Fig. 8F). Because the endogenous β-gal activity in the kidney of wild type animals is barely detectable at this stage (Fig. 5), wild type control samples were omitted from this experiment. Again, ISH with the antisense probe revealed a similar pattern in $Af17^{+/+}$ mice to that of the X-gal staining in $Af17^{-/-}$ mice. The corresponding sense probe yielded very low background only (Fig. 8H). In brief, the X-gal staining apparently mimics the expression pattern of the endogenous Af17 mRNA expression as defined by ISH.

Discussion

Using a gene trap approach, we have generated the first Af17 mutant mouse model and found that homozygous mutant animals are viable, fertile and do not have readily observable phenotypes. The absence of overt phenotype in $Af17^{-/-}$ mice may be due to redundancy of other proteins, such as AF10 or BR140 of the same protein family. In support of this idea, AF10 (Linder *et al.*, 1998) and BR140 (Thompson *et al.*, 1994) are also predominantly expressed in the testis and other tissues, where Af17 is also expressed (Figs. 5 and 6). Alternatively, but not exclusively, the PHD-finger-harboring segment (aa 1 - 255) of Af17 retained in the Af17-β-geo fusion protein plays a critical role for the survival and normal development of the animal, raising the possibility that the mutant mice may not carry a true null allele. However, since the majority of Af17 sequence containing all other domains was already deleted, including the DNA binding domains and the area binding to Dot1, we do not favor this possibility. We could not find other instances from the literature that a single PHD finger domain rescues the knockout phenotype, either.

The Mll1-Af17 fusion protein is leukemogenic. As a general rule, although individual fusion partners may determine the phenotype of resulting leukemias, they do not necessarily possess specific functions in hematopoietosis (Liu *et al.*, 2009). Accordingly, it is not surprising that Af17 may not be required for normal hematopoietosis and actually may not even be expressed in the bone marrow. Similar to our investigation, no effect on hematopoiesis was observed in the transgenic mouse with a null mutation of Af9 (Collins *et al.*, 2002), a very common fusion partner of Mll1 and a competitor of Af17 for binding with Dot1 (Reisenauer *et al.*, 2009). Nevertheless, there may be defects in early stem and/or progenitor cell development in Af17 mutant animals and that with time, the cell numbers and respective percentages could normalize. Accordingly, the possibility that Af17 plays a role in hematopoiesis can not be completely ruled out.

Outside of the hematopoietic system, the expression pattern of Af17 strongly indicates it has functions in the nervous system, heart and kidney. In the nervous system, Af17 expression is observed continuously from early embryonic to adult stages, which suggests that Af17 is functional in both proliferating and differentiated neurons.

Based on the very specific expression pattern of Af17 in the nervous system, especially during the embryonic stage, some of its functions may be implied. The earliest Af17 expression is mainly observed in the MHJ of embryos. This region is a well-recognized organizer that controls the anterior-posterior patterning of the developing midbrain and hindbrain. In this area, multiple interconnecting pathways have been identified, including Fgfs, Wnts, and many others. Our data show that the Af17 expressing area in MHJ is very similar to that of Fgf8 (Lee *et al.*, 1997) or Wnt1 (Wilkinson *et al.*, 1987). Since Af17 is putatively a transcription factor and remains in the cell, instead of being a secreted morphogen, it probably lies downstream of those organizing molecules. In agreement with this idea, it has been reported that Af17 transcription responds to the level of APC (Lin *et al.*, 2001), a regulator of β-catenin, the latter in turn is the most critical component of the Wnt signaling transduction. Af17 also forms a complex with β–catenin (Mohan *et al.*), so it seems that Af17 can be interacting at multiple places along the signaling transduction pathway. Besides Wnts, it is generally accepted that Fgf8 is the most important organizing molecule emanated from the MHJ, so it will be interesting to test direct relations between Af17 and Fgf8 pathway components.

The wide expression pattern of Af17 in kidney indicates that it may play an important role in renal physiology. We previously proposed that Af17 competes with Af9 for binding to Dot1a, a methyltransferase highly specific for histone H3 lysine 79, and relieves Dot1a-mediated repression of several aldosterone regulated genes including those encoding the epithelial Na^+ channel subunits in 293T cells (Reisenauer *et al.*, 2009). Indeed, while *Af17*$^{-/-}$ mice do not show obvious morphological abnormalities, they have an impaired ability to retain renal water and electrolytes (unpublished data).

Methods

Reagents

An anti-Af17 antibody was generated by immunizing chicken with a peptide corresponding to mouse Af17 aa 257-270 (GenBanK access number: AY050217), and affinity-purified using the corresponding peptide (New England Peptide Inc). Three additional commercial Af17 antibodies were obtained from Abcam, Abnova, and Bethyl. Antibodies for detection of β-galactosidase were acquired from Abcam, Novus and Promega. Anti-GFAP and anti-NeuN antibodies were purchased from DAKO and Chemicon, respectively. A PCR fragment encoding Af17 aa 237-387 was amplified with RIKEN EST clone (GenBank access number: BB729800) was cloned into pGEM3 at EcoRI/XhoI to generate pGEM3-Af17 aa 237-387.

Generation and characterization of Af17 gene trap mice

The ES cell line used for this research project, SIGTR AC0433, identification number 020107-UCD, was obtained from the Mutant Mouse Regional Resource Center (MMRRC), an NCRR-NIH funded strain repository, and was donated to the MMRRC by the NHLBI-funded research consortium, Sanger International Gene Trap Center (http://www.sanger.ac.uk/PostGenomics/genetrap/). The ES cells were injected into C57BL/6 blastocysts at the Transgenic Knock-out Core Facility, The Brown Foundation Institute of Molecular Medicine for the Prevention of Human Diseases, The University of Texas Health Science Center at Houston. Male chimeras were bred to C57BL/6 for germline transmission. Mice were genotyped by PCR with yolk sac, toe, or tail genomic DNA. Sequences of the

primer sets used for PCR were: GCTTCTTTCCAGAGACCGCCACCAG and CACACACCCGCACGCCATACAGTCC for the mutant *Af17* allele, GCTTCTTTCCAGAGACCGCCACCAG and CCTGTCCCATTATCGTGCCAGTGAC for the WT *Af17* allele. All animal experiments were performed according to institutional guidelines.

Detection of transgenic β-galactosidase activity (X-gal staining)

Embryos and adult tissues were fixed in freshly prepared 4% paraformaldehyde at room temperature for 30-60 minutes depending on size, rinsed in rinsing buffer (PBS with 0.02% NP-40, 0.01% sodium deoxycholate, and 2mM $MgCl_2$) and then incubated in staining solution (1 mg/ml X-gal plus 5 mM potassium ferricyanide and 5 mM potassium ferrocyanide in rinsing buffer) overnight at 37°C. After rinsing briefly, the embryos and tissues were post-fixed in 4% paraformaldehyde for 30 minutes, rinsed and then stored in PBS for photography as whole mount samples. When sections were made to reveal inner structures, stained embryos were frozen with Optimal Cutting Temperature (OCT) embedding medium, sectioned with a cryostat and photographed with a microscopic system. Adult tissues were quickly frozen with liquid nitrogen and embedded in OCT for sectioning. Sections of adult tissues were fixed and X-gal stained. Nuclear fast red or brazilin counterstaining was used to yield a clear contrast for sections. For X-gal staining of bone marrow smears, bone marrow from femurs was spread on microscopic slides and air dried. The smears were fixed, X-gal stained and counterstained as described for fresh frozen sections.

RT-PCR

RT-PCR was performed as previously described with tissues isolated from 6-8 week-old mice (Zhang *et al.*, 2006). WT *Af17* mRNA was amplified with primers GGGCTTCTGGGAGGGTTGAATG and AAGGGTTGGTCTGAGCAGTGAGGAC. The mutant *Af17* mRNA was detected with primers CAGTAGTGCCAGCGGTGGTGGAGG and AGTATCGGCCTCAGGAAGATCG.

In situ hybridization (ISH)

ISH was performed with RNA probes labeled by digoxigenin. The probes were synthesized with a DIG RNA labeling kit with pGEM3-Af17 aa 237-387 as the template and post-hybridization detection was performed with a DIG nucleic acid detection kit (both from Roche) according to manufacturer's instructions.

Immunohistochemistry

Immunohistochemical labeling was performed on slides after X-gal staining. Primary antibodies (anti-GFAP and anti-NeuN) were diluted with PBS plus 5% normal serum (based on the animal species of the secondary antibody) and incubated with the slides overnight at 4°C. HRP labeled secondary antibody, Elite ABC kit, and DAB staining kit (all from Vector Lab) were used for subsequent immunostaining procedures according to the manufacturer's instructions.

Blood analyses

Blood smears were made using tail blood of 6-week mice. The smear was dried at room temperature for 15 minutes and stained by WG16-500ml kit (Sigma-Aldrich) according to the manufacturer's instructions. For complete blood count, blood was collected from isoflurane anesthetized mice by heart puncture, and analyzed with the Forcyte Veterinary Hematology System (Oxford Science, Inc).

Statistical analysis

All quantitative data are presented as mean±SEM. The statistical significance between WT and *Af17*$^{-/-}$ for each parameter was determined by Student t-test, with significance level set at $P<0.05$.

Supplementary Material

Refer to Web version on PubMed Central for supplementary material.

Acknowledgments

We thank Dr. Eva M. Zsigmond for microinjection of the ES cells and production of the chimera mice. This work was funded by American Heart Association Beginning Grant-in-Aid 0865271F (to W.Z.), American Society of Nephrology Carl W. Gottschalk Research Scholar Grant (to W.Z.), and National Institutes of Health grants R01 DK080236 (to W.Z.).

References

Bach C, Slany RK. Molecular pathology of mixed-lineage leukemia. Future Oncol. 2009; 5:1271–1281. [PubMed: 19852741]

Bahri SM, Chia W, Yang X. The Drosophila homolog of human AF10/AF17 leukemia fusion genes (Dalf) encodes a zinc finger/leucine zipper nuclear protein required in the nervous system for maintaining EVE expression and normal growth. Mech Dev. 2001; 100:291–301. [PubMed: 11165485]

Beverloo HB, Le Coniat M, Wijsman J, Lillington DM, Bernard O, de Klein A, van Wering E, Welborn J, Young BD, Hagemeijer A, et al. Breakpoint heterogeneity in t(10;11) translocation in AML-M4/M5 resulting in fusion of AF10 and MLL is resolved by fluorescent in situ hybridization analysis. Cancer Res. 1995; 55:4220–4224. [PubMed: 7671224]

Chaplin T, Ayton P, Bernard OA, Saha V, Della Valle V, Hillion J, Gregorini A, Lillington D, Berger R, Young BD. A novel class of zinc finger/leucine zipper genes identified from the molecular cloning of the t(10;11) translocation in acute leukemia. Blood. 1995; 85:1435–1441. [PubMed: 7888665]

Collins EC, Appert A, Ariza-McNaughton L, Pannell R, Yamada Y, Rabbitts TH. Mouse Af9 is a controller of embryo patterning, like Mll, whose human homologue fuses with Af9 after chromosomal translocation in leukemia. Mol Cell Biol. 2002; 22:7313–7324. [PubMed: 12242306]

Crosby MA, Miller C, Alon T, Watson KL, Verrijzer CP, Goldman-Levi R, Zak NB. The trithorax group gene moira encodes a brahma-associated putative chromatin-remodeling factor in Drosophila melanogaster. Mol Cell Biol. 1999; 19:1159–1170. [PubMed: 9891050]

Eng LF, Ghirnikar RS, Lee YL. Glial fibrillary acidic protein: GFAP-thirty-one years (1969-2000). Neurochem Res. 2000; 25:1439–1451. [PubMed: 11059815]

Kleiter N, Artner I, Gmachl N, Ghaffari-Tabrizi N, Kratochwil K. Mutagenic transgene insertion into a region of high gene density and multiple linkage disruptions on mouse chromosome 11. Cytogenet Genome Res. 2002; 97:100–105. [PubMed: 12438746]

Lee SM, Danielian PS, Fritzsch B, McMahon AP. Evidence that FGF8 signalling from the midbrain-hindbrain junction regulates growth and polarity in the developing midbrain. Development. 1997; 124:959–969. [PubMed: 9056772]

Lin YM, Ono K, Satoh S, Ishiguro H, Fujita M, Miwa N, Tanaka T, Tsunoda T, Yang KC, Nakamura Y, Furukawa Y. Identification of AF17 as a downstream gene of the beta-catenin/T-cell factor pathway and its involvement in colorectal carcinogenesis. Cancer Res. 2001; 61:6345–6349. [PubMed: 11522623]

Linder B, Jones LK, Chaplin T, Mohd-Sarip A, Heinlein UA, Young BD, Saha V. Expression pattern and cellular distribution of the murine homologue of AF10. Biochim Biophys Acta. 1998; 1443:285–296. [PubMed: 9878787]

Liu H, Cheng EH, Hsieh JJ. MLL fusions: pathways to leukemia. Cancer Biol Ther. 2009; 8:1204–1211. [PubMed: 19729989]

Lonie A, D'Andrea R, Paro R, Saint R. Molecular characterisation of the Polycomblike gene of Drosophila melanogaster, a trans-acting negative regulator of homeotic gene expression. Development. 1994; 120:2629–2636. [PubMed: 7956837]

Mohan M, Herz HM, Takahashi YH, Lin C, Lai KC, Zhang Y, Washburn MP, Florens L, Shilatifard A. Linking H3K79 trimethylation to Wnt signaling through a novel Dot1-containing complex (DotCom). Genes Dev. 24:574–589. [PubMed: 20203130]

Mullen RJ, Buck CR, Smith AM. NeuN, a neuronal specific nuclear protein in vertebrates. Development. 1992; 116:201–211. [PubMed: 1483388]

Musselman CA, Kutateladze TG. PHD fingers: epigenetic effectors and potential drug targets. Mol Interv. 2009; 9:314–323. [PubMed: 20048137]

Okada Y, Feng Q, Lin Y, Jiang Q, Li Y, Coffield VM, Su L, Xu G, Zhang Y. hDOT1L links histone methylation to leukemogenesis. Cell. 2005; 121:167–178. [PubMed: 15851025]

Prasad R, Leshkowitz D, Gu Y, Alder H, Nakamura T, Saito H, Huebner K, Berger R, Croce CM, Canaani E. Leucine-zipper dimerization motif encoded by the AF17 gene fused to ALL-1 (MLL) in acute leukemia. Proc Natl Acad Sci U S A. 1994; 91:8107–8111. [PubMed: 8058765]

Reisenauer MR, Anderson M, Huang L, Zhang Z, Zhou Q, Kone BC, Morris AP, Lesage GD, Dryer SE, Zhang W. AF17 Competes with AF9 for Binding to Dot1a to Up-regulate Transcription of Epithelial Na+ Channel {alpha}. J Biol Chem. 2009; 284:35659–35669. [PubMed: 19864429]

Slany RK. The molecular biology of mixed lineage leukemia. Haematologica. 2009; 94:984–993. [PubMed: 19535349]

Thompson KA, Wang B, Argraves WS, Giancotti FG, Schranck DP, Ruoslahti E. BR140, a novel zinc-finger protein with homology to the TAF250 subunit of TFIID. Biochem Biophys Res Commun. 1994; 198:1143–1152. [PubMed: 7906940]

Vogel T, Gruss P. Expression of Leukaemia associated transcription factor Af9/Mllt3 in the cerebral cortex of the mouse. Gene Expr Patterns. 2009; 9:83–93. [PubMed: 19000783]

Wilkinson DG, Bailes JA, McMahon AP. Expression of the proto-oncogene int-1 is restricted to specific neural cells in the developing mouse embryo. Cell. 1987; 50:79–88. [PubMed: 3594565]

Zhang W, Hayashizaki Y, Kone BC. Structure and regulation of the mDot1 gene, a mouse histone H3 methyltransferase. Biochem J. 2004; 377:641–651. [PubMed: 14572310]

Zhang W, Xia X, Jalal DI, Kuncewicz T, Xu W, Lesage GD, Kone BC. Aldosterone-sensitive repression of ENaCalpha transcription by a histone H3 lysine-79 methyltransferase. Am J Physiol Cell Physiol. 2006; 290:C936–946. [PubMed: 16236820]

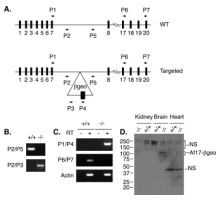

Fig. 1. Generation of *Af17*$^{-/-}$ mice

A. Diagrams showing the WT and targeted *Af17* loci. An *Af17*-specific gene trap ES clone (GenBank# CW988924) was used for generation of *Af17*$^{-/-}$ mice. In these cells, the gene trap vector carrying βgeo reporter was inserted into intron 7 as shown. The exact insertion site was found 257 bp downstream from the start of intron 7 (GenBank # GU271153). The relative location and orientation of each primer used for genotyping are also indicated. ***B.*** A representative agarose gel image showing PCR-based genotyping of genomic DNA. PCR was conducted with primers indicated to amplify a 373-bp WT or 542-bp mutant fragment in separate reactions. ***C.*** A representative agarose gel image confirming the disruption of *Af17* mRNA. Total RNA was isolated from adult WT and mutant brains and analyzed by RT-PCR in the absence or presence of the reverse transcriptase (RT), with the primers indicated, to amplify 498-bp WT or 467-bp mutant cDNA fragments in separate reactions. *β-actin* was used as a control of the RT-PCR conditions. ***D.*** A representative immunoblot confirming the expression of the Af17-βgeo fusion protein. Total kidney, brain, or heart lysates from four WT (n=4 mice) and three (n=3 mice) mutant mice were prepared. Samples from the same tissue of the same genotype were combined and analyzed by immunoblotting with a chicken antibody recognizing β-galactosidase (Abcam). NS: non-specific.

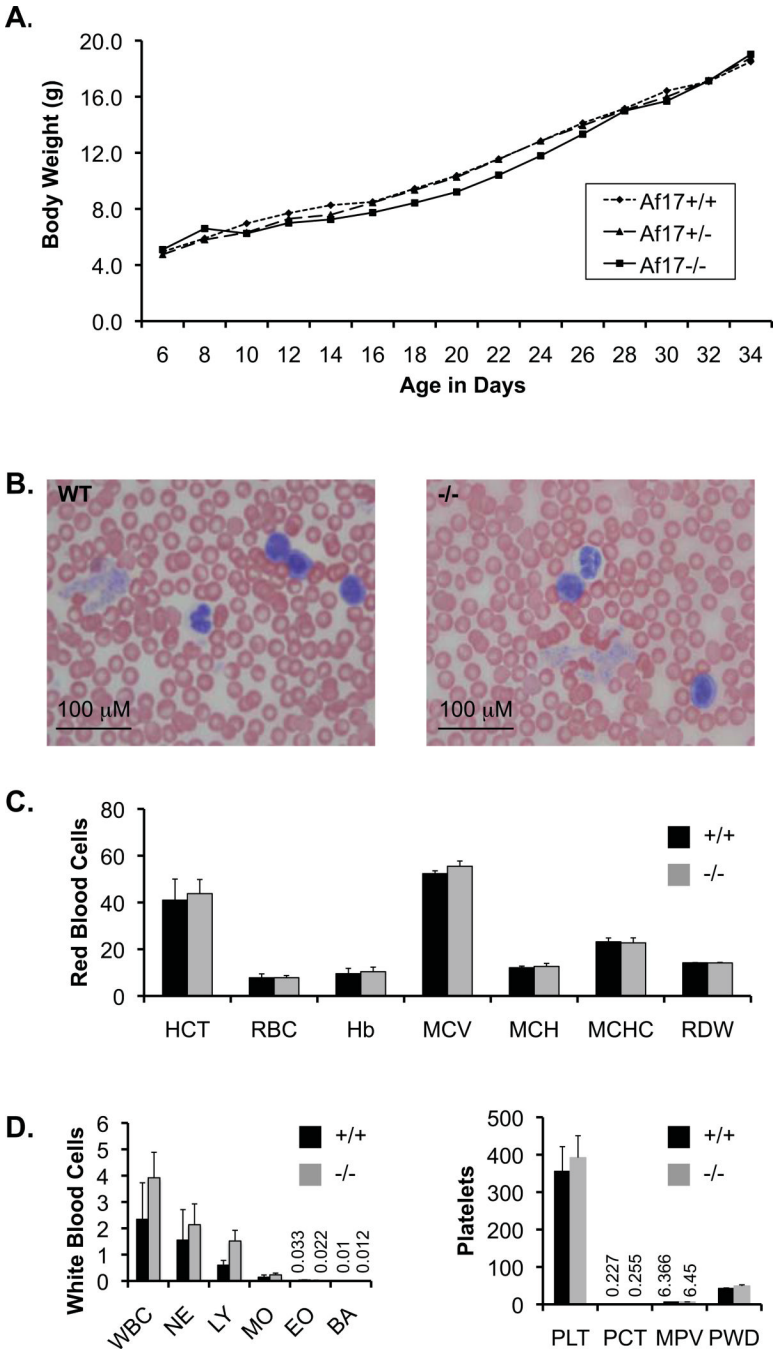

Fig. 2. *Af17*$^{-/-}$ animals do not display obvious abnormality in growth rate and peripheral blood morphology

A. Shown is a growth curve plotting body weight (g) vs age in days. Body weights of WT (n=8 mice), *Af17*$^{+/-}$ (n=14 mice) and *Af17*$^{-/-}$ (n=10 mice) were recorded every other day as indicated. No significance between any two genotypes at any given time point was observed. For simplicity, SEM is not shown. Each SEM is less than 20% of the means. ***B.*** Representative images of peripheral blood smears revealing no abnormal blood cells from WT (n=5 mice) and *Af17*$^{-/-}$ animals (n=5 mice). Areas where cells did not overlap were randomly picked, at least 10 fields examined and pictures taken. ***C-E***. Complete blood count. Shown are means ± SEM of various blood parameters from 6-8 week old WT (n= 3

mice) and *Af17*$^{-/-}$ mice (n= 8 mice) as indicated. HCT: hematocrit (%); RBC: red blood cells (10^6/μL); Hb: hemoglobin (g/dL); MCV: mean corpuscular (erythrocyte) volume (fL); MCH: mean corpuscular hemoglobin (pg); MCHC: mean corpuscular hemoglobin concentration (g/dL); RDW: red cell (erythrocyte volume) distribution width (%); WBC: white blood cell (leukocyte count) (10^3/μL); NE, LY, MO, EO, and PA: absolute number of neutrophils, lymphocytes, monocytes, eosinophils, and basophils (10^3/μL), respectively; PLT: platelet (thrombocyte count) (10^3/μL); PCT: platelet crit. MPV: mean platelet volume (fL); PWD: platelet distribution width.

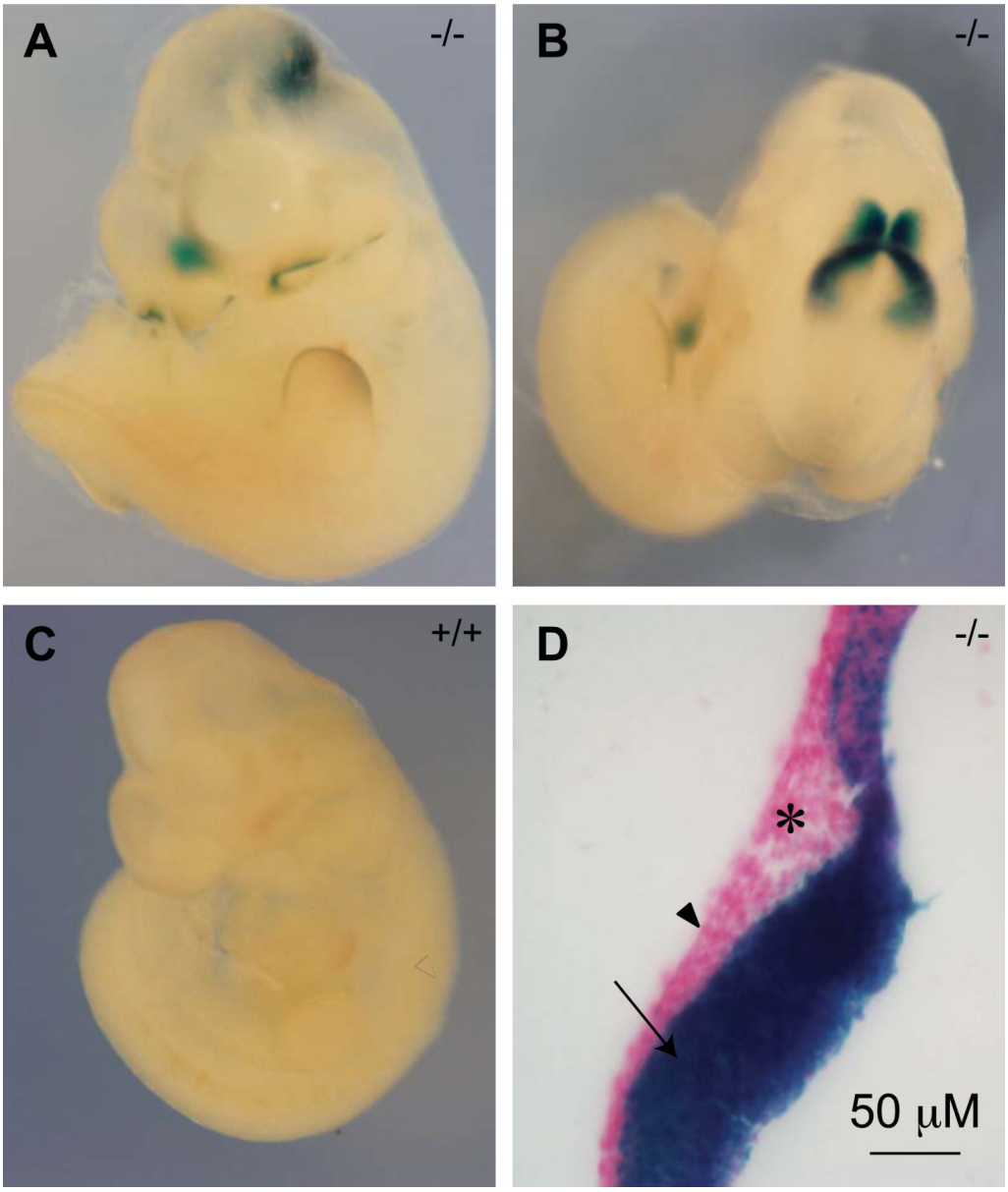

Fig. 3. *Af17* promoter activity detected by X-gal staining in E10.5 day embryos

A*-*B. An *Af17*$^{-/-}$ E10.5 embryo shown from side (***A***) and top aspects (***B***). X-gal staining is seen in the midbrain-hindbrain junction area (HMJ, or isthmus), margin of the olfactory pit, and the median portion of the most rostral end of the developing forebrain, and tail bud. In addition, weaker staining is seen at the edge of the forelimb bud. ***C***. A WT littermate embryo shown from side aspect with no X-gal staining seen. ***D.*** A representative sagittal section of the *Af17*$^{-/-}$ embryo showing that the expression is limited to the neuroepithelium (arrow). No obvious staining is observed in the ectoderm (arrowhead) and mesoderm (asterisk).

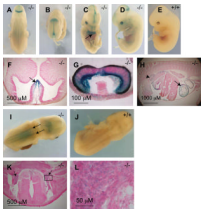

Fig. 4. X-gal staining in E12.5 and E14.5 day *Af17*$^{-/-}$ embryos

A-C. At E12.5 day, X-gal staining is seen in the MHJ (***A***), along the middle of the roof of the midbrain (***B***) and the median walls of telencephalic vesicles (***C***). ***D.*** Developing optic vesicle begins to show x-gal staining at E12.5 day. ***E.*** A wild type embryo showing lack of X-gal staining at E12.5 day. ***F-G*** transverse sections confirmed X-gal staining in the median wall of the telencephalic vesicles (***F***, arrow), eye primordium (***G***), heart (***H***, arrow, also ***C***, arrow), and the metanephrone i.e. the developing kidney (***H***, arrowhead). ***I.*** An E14.5 day *Af17*$^{-/-}$embryo showing the dorsal root ganglia clearly X-gal stained (arrows). ***J***. A WT E14.5 littermate embryo showing no X-gal staining. ***K***. A transverse section showing the X-gal staining in the dorsal root ganglia (arrows). ***L.*** A high magnification image of the boxed area in ***K***.

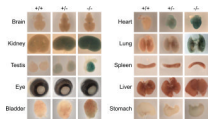

Fig. 5. Whole mount X-gal staining of embryonic organs

As in Fig. 4 except various organs isolated from E16.5 day embryos of the three genotypes as indicated.

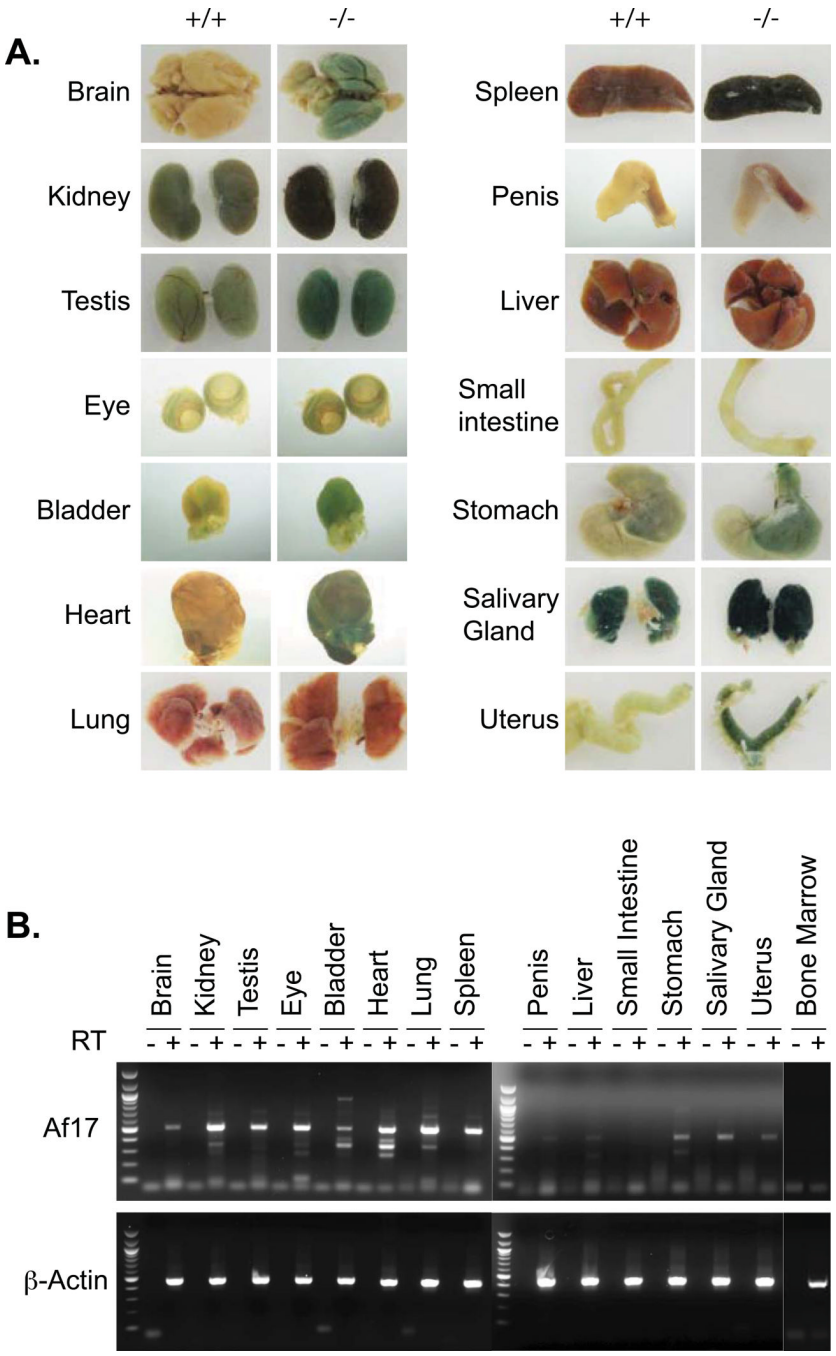

Fig. 6. *Af17* expression in adult organs

A. Shown is whole mount X-gal staining of adult organs. As in Fig. 5 except that organs were isolated from 6-8 week old *Af17*$^{-/-}$mice and their WT littermates. ***B.*** As in ***A*** and Fig. 1C, organs were isolated from adult WT animals and examined for *Af17* mRNA expression by RT-PCR, with *β-actin* as internal control, followed by agarose gel analyses.

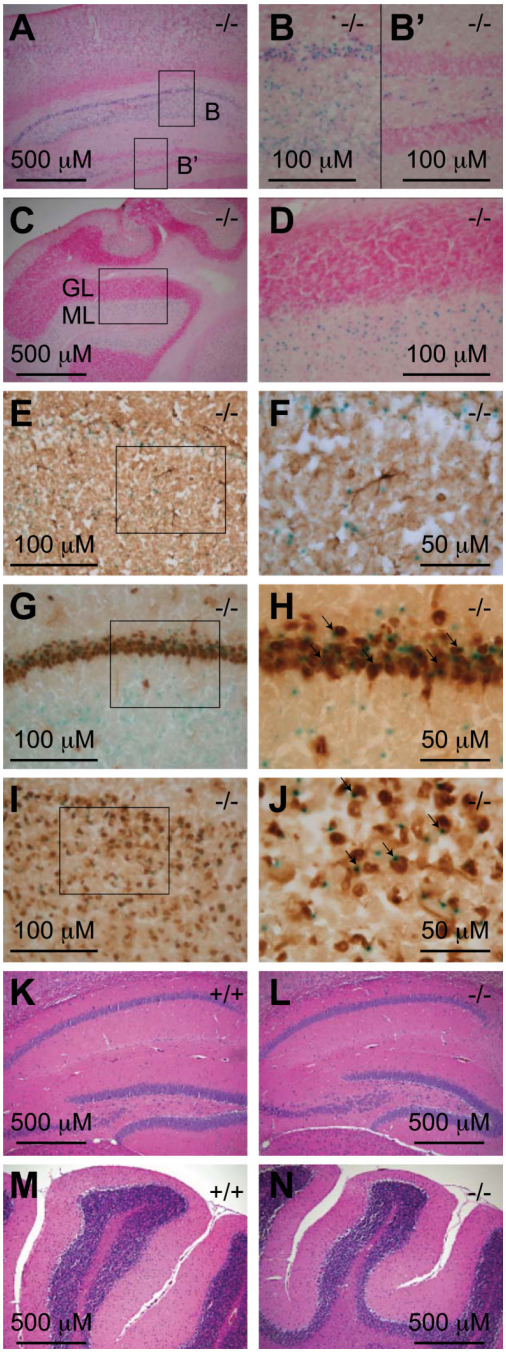

Fig. 7. Af17 is expressed in the neurons of adult animals

A. X-gal staining of a sagittal brain section from an *Af17*$^{-/-}$ animal with stained cells in the cerebral cortex and the CA areas of the hippocampus. ***B*** & ***B'***. High magnification images of the boxed areas in ***A***. Note the staining in the CA areas but not in the dental gyrus. ***C.*** X-gal staining of a sagittal brain section from an *Af17*$^{-/-}$ mouse showing stained cells in the cerebellum. GL: granular layer; ML: molecular layer. ***D.*** A high magnification image of the boxed area in ***C***. Sections in ***A-D*** were counterstained with nuclear fast red. ***E.*** Immunohistochemical (IHC) staining for GFAP in a transverse brain section after X-gal staining. Note that the blue X-gal staining and the brown IHC staining do not coexist in the same cells. ***F.*** A higher magnification image of the boxed area in ***E***. ***G-J.*** IHC staining for

NeuN and X-gal staining in a transverse brain section showing the hippocampal CA areas (***G***) and the cerebral cortex (***I***), with higher magnification images of their boxed areas shown in ***H*** and ***I***, respectively. Note the cells stained by both X-gal and IHC (arrows). ***K-N***. Hematoxylin & Eosin staining of sagittal brain sections from 6-8 week old WT (***K*** & ***M***) and *Af17*$^{-/-}$ (***L*** & ***N***) animals showing similar morphology of the hippocampus (***K*** & ***L***) and the cerebellum (***M*** & ***N***). All animals shown were 6 weeks old.

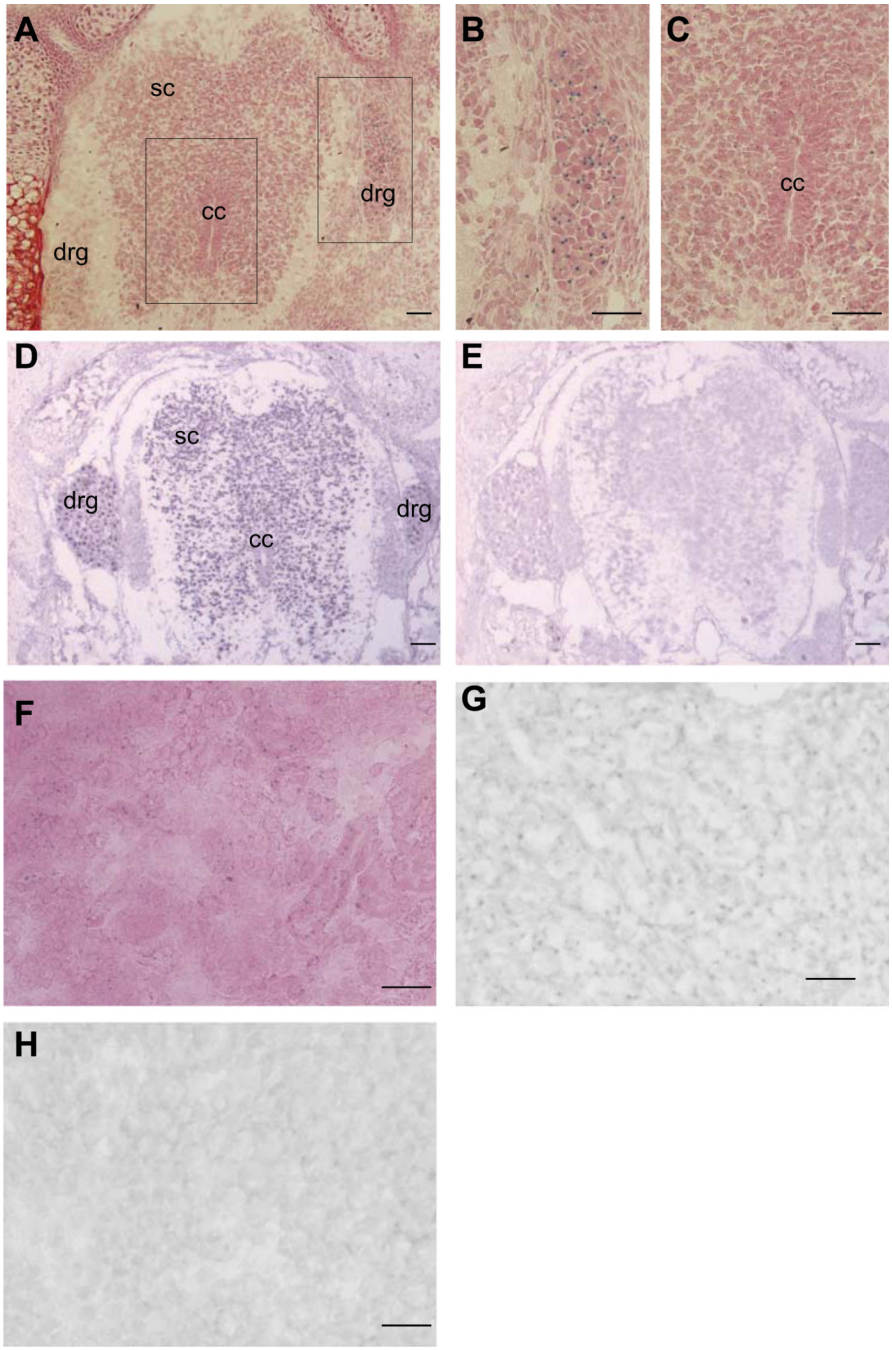

Fig. 8. Af17 mRNA expression pattern detected by in situ hybridization imitates X-gal staining pattern

A. X-gal staining performed on a transverse section of an E17.5 *Af17*$^{-/-}$ embryo. An area around the spinal cord and the DRG is shown. Strong staining was observed in the DRG, and relatively weaker staining in the spinal cord. Boxed areas were enlarged and shown in panel ***B*** **and** ***C. D.*** In situ hybridization with an Af17-specific anti-sense probe. Signals are identified in the spinal cord and DRG. Very little staining was located in surrounding tissue. ***E.*** In situ hybridization with the corresponding sense probe. No clear signal can be identified. ***F.*** X-gal staining performed on a kidney section of an E17.5 *Af17*$^{-/-}$ embryo. Signals can be localized in both cortex and medulla. ***G*** and ***H***. In situ hybridization

performed on kidney sections with the anti-sense or sense probes. Only the anti-sense probe yielded signals (***G***), no signal was identified with the sense probe. The sections were counter-stained with brazilin. drg: dorsal root ganglion; sc: spinal cord; cc: central canal. Scale bar: 50 μm.